TECHNICAL REPORTS

nature medicine

Molecular modeling, organ culture and reverse genetics for a newly identified human rhinovirus C

Yury A Bochkov[1], Ann C Palmenberg[2], Wai-Ming Lee[1], Jennifer A Rathe[3], Svetlana P Amineva[1], Xin Sun[4], Thomas R Pasic[5], Nizar N Jarjour[6], Stephen B Liggett[3] & James E Gern[1,6]

A recently recognized human rhinovirus species C (HRV-C) is associated with up to half of HRV infections in young children. Here we propagated two HRV-C isolates *ex vivo* in organ culture of nasal epithelial cells, sequenced a new C15 isolate and developed the first, to our knowledge, reverse genetics system for HRV-C. Using contact points for the known HRV receptors, intercellular adhesion molecule-1 (ICAM-1) and low-density lipoprotein receptor (LDLR), inter- and intraspecies footprint analyses predicted a unique cell attachment site for HRV-Cs. Antibodies directed to binding sites for HRV-A and -B failed to inhibit HRV-C attachment, consistent with the alternative receptor footprint. HRV-A and HRV-B infected HeLa and WisL cells but HRV-C did not. However, HRV-C RNA synthesized *in vitro* and transfected into both cell types resulted in cytopathic effect and recovery of functional virus, indicating that the viral attachment mechanism is a primary distinguishing feature of HRV-C.

HRVs are positive-strand RNA viruses in the family *Picornaviridae*. They share a common genome organization, and isolates are typically classified into one of three species (A, B and C) according to phylogenetic sequence criteria[1]. HRV is the most frequent cause of the common cold, but recent data have shown that HRV infection has pathogenic potential beyond rhinosinusitis. It is now recognized that 50–85% of asthma exacerbations are due to HRV infections[2–4], and wheezing illnesses in infancy caused by HRV are associated with a high risk of developing childhood asthma[5]. HRV infections of all types are major contributors to morbidity associated with exacerbations of other chronic lung diseases such as cystic fibrosis and chronic obstructive pulmonary disease[6,7].

Recently, partial or full genome sequencing has been used to place clinical isolates within the 99 types of HRV-A and HRV-B. However, some cases, often associated with children hospitalized with lower respiratory tract disease, began to appear where the identified HRV sequences were not consistent with those of known HRV types[8–14]. Full-genome sequencing has shown the distinct nature of these HRVs, which are now designated as HRV-C[1,15,16]. The pathogenesis and antigenic variability associated with HRV-C, the mechanism of viral attachment to host cells and potential treatments have been elusive because, unlike HRV-A and HRV-B, HRV-C has not been successfully propagated in any cell type *in vitro*[17].

To address these fundamental questions about HRV-C biology, it was first necessary to develop a functional culture system. We now report the characterization and complete genome sequencing of an HRV-C isolate (HRV-C15 type) that can be grown in mucosal organ culture. Bioinformatic comparisons of this new genome and other HRV-C sequences showed unique composition profiles in the putative ICAM-1 and LDLR footprint locales, inconsistent with all known major and minor group virus-receptor interactions. Full-length HRV-C15 RNA synthesized *in vitro* from a cDNA clone was infectious when transfected into cultured cell lines. We have used this methodology to initiate descriptions of the virus's biology, tissue tropism, the replication cycle and response to antiviral and antireceptor compounds.

RESULTS

HRV-C amplification in sinus mucosal organ culture

We introduced several specimens of nasal lavage fluid (NLF) with high copy number of HRV-C RNA into multiple human fibroblast and epithelial cell lines (WI-38, WisL, BEAS-2B, A549 and HeLa) susceptible to HRV-A and HRV-B infection and primary cultures of human lung fibroblasts and bronchial, sinus and adenoidal epithelial cells from several donors. Primary epithelial cultures included cell monolayers, differentiated cells (air-liquid interface method) and primary bronchial epithelial (PBE) cells treated with interleukin-13 to induce goblet cell metaplasia. Assigning an increase in the quantitative RT-PCR (qRT-PCR) signal as an indicator of HRV-C replication, we were successful in none of these attempts, including those where multiple serial blind passages were undertaken.

Reasoning that organ culture might best mimic natural replication circumstances, we cultured surgery-derived byproduct tissues (from multiple anonymous donors) from sinus mucosa, adenoids, tonsils and nasal polyps. After 1–3 d, viable tissues (continuous ciliary activity) negative for common respiratory viral pathogens were inoculated with representative laboratory HRV-A strains that use ICAM-1 (A16)

[1]Department of Pediatrics, University of Wisconsin School of Medicine and Public Health, Madison, Wisconsin, USA. [2]Institute for Molecular Virology, University of Wisconsin–Madison, Madison, Wisconsin, USA. [3]Cardiopulmonary Genomics Program, University of Maryland School of Medicine, Baltimore, Maryland, USA. [4]Laboratory of Genetics, University of Wisconsin–Madison, Madison, Wisconsin, USA. [5]Department of Surgery, University of Wisconsin School of Medicine and Public Health, Madison, Wisconsin, USA. [6]Department of Medicine, University of Wisconsin School of Medicine and Public Health, Madison, Wisconsin, USA. Correspondence should be addressed to Y.A.B. (yabochkov@wisc.edu).

Received 6 July 2010; accepted 1 December 2010; published online 10 April 2011; doi:10.1038/nm.2358

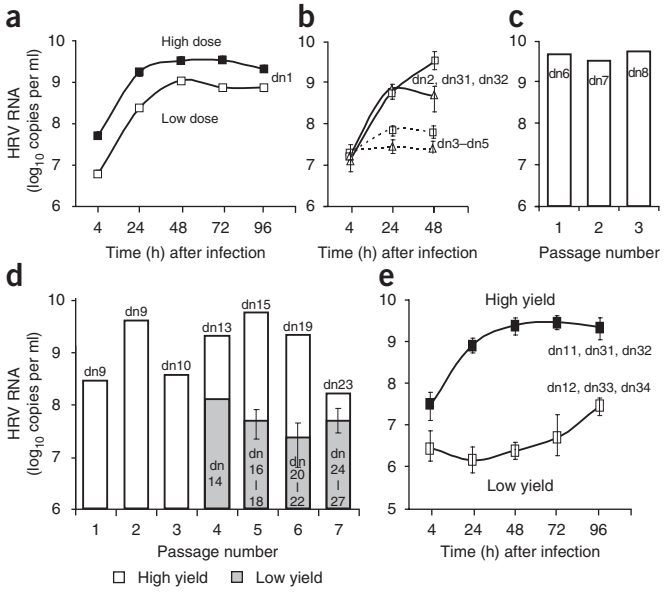

Figure 1 Propagation of HRV in mucosal organ cultures. (**a**) Viral replication in single sinus organ culture infected with either high or low doses of HRV-A16. (**b**) Growth curve of HRV-A1 (triangles) and HRV-A16 (squares) strains in organ cultures after inoculation (1×10^9 vRNA copies per ml) of sinus (solid lines) versus adenoidal (dashed lines) tissue (means ± s.d.). (**c**) Serial propagation (72 h) of a clinical isolate (HRV-A78) in three successive sinus organ cultures. (**d**) Propagation of HRV-C15 in sinus mucosal organ cultures. Cultured sinus tissue (passage 1) was inoculated with NLF containing HRV-C15, and serially passaged (passages 2–7), resulting in either high (≥2×10^8 vRNA copies per ml) or low viral yields. (**e**) Growth curve of HRV-C15 (means, ± s.d.) in sinus organ cultures revealing distinct replication kinetics and viral yields. Organ cultures are designated according to tissue donors (dn).

or LDLR (A1) for cell attachment. Sinus mucosal cultures inoculated with HRV-A16 (1×10^9 viral RNA (vRNA) copies per ml) increased viral RNA by up to 100 fold, even at low (1×10^8 vRNA copies per ml) dose (**Fig. 1a**). Repeated tests with tonsils and nasal polyps (data not shown) and adenoid tissues (**Fig. 1b**) showed lower (fivefold or less) increase in vRNA. Furthermore, a NLF specimen containing 2×10^8 vRNA copies per ml of a field HRV-A isolate (A78) responded similarly to laboratory strains and we passaged it serially into three tissue specimens (**Fig. 1c**).

Using this approach, we inoculated an HRV-C15 isolate from a specimen of NLF (2.6×10^8 vRNA copies per ml) into sinus organ culture, and high-level viral replication was maintained through seven serial passages (**Fig. 1d**). During each passage, we observed partial inhibition of ciliary beating at 48–72 h, coinciding with the peak of virus replication, but we noted no other specific cytopathic effects. When we used similar doses (1×10^9 vRNA copies per ml) of HRV-C15 (**Fig. 1e**) and HRV-A16 (**Fig. 1a**) for infection, the growth kinetics were equivalent to each other in high-yield cultures. Serial passage of a second HRV-C isolate (W23)[10] was also accomplished by a similar approach (data not shown). Our attempts to adapt these isolates grown in organ culture to multiple cell lines (listed above) were not successful.

HRV-C localization in sinus epithelium

We analyzed HRV-C15 replication in sinus tissues by *in situ* hybridization using whole-mount procedures and a digoxigenin-labeled RNA probe specific for the HRV-C15 plus-strand RNA. We observed positive hybridization in both of the inoculated sinus organ cultures, but it was absent in the mock-infected cultures (**Fig. 2a**). Higher-resolution images showed a patchy distribution of HRV-C15–positive cells with the highest signal intensities at the edges of tissues (**Fig. 2b**), suggesting

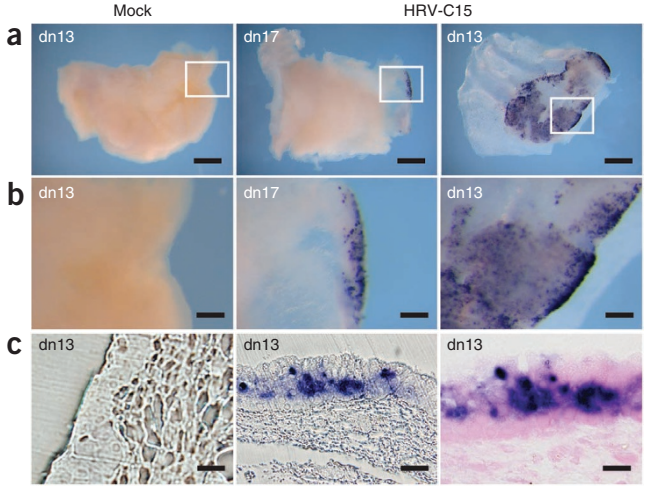

that mechanical injury may increase susceptibility to infection, perhaps by exposing subapical epithelial layers expressing virus receptors.

The two tissue specimens inoculated with HRV-C15 differed in signal intensity and corresponding virus yield. In the tissue (dn17) with the lower yield (1×10^7 vRNA copies per ml) the RNA signal was limited to small area at the fragment edge, whereas the higher-yield tissue (dn13, 2×10^9 vRNA copies per ml) gave many foci, with a greater total density of infected cells (**Fig. 2b**). In tissue cross sections, the positive signals originated mainly from middle and upper epithelial layers (**Fig. 2c**). An outermost sloughing of ciliated cells (**Fig. 2c**) was particularly apparent in the higher-titer tissues. There was no evidence for infection of cells deeper than the epithelial layer in either sample.

Genome analysis of HRV-C15

From the organ culture supernatant fluid (passage 4), we sequenced the complete HRV-C15 genome consisting of 7,111 bases. The single open reading frame encodes a polyprotein of 2,153 amino acids (the longest among the reported HRV-C strains), flanked by 5′ and 3′ untranslated regions (UTR) of 607 and 45 nucleotides, respectively. The RNA and deduced polyprotein sequences share characteristic HRV-C features such as a putative internal *cis*-acting replication element (*cre*) located within viral protein 2 (VP2) (1B), a Met67-Ser68 cleavage site at the VP4-VP2 junction, species-specific insertions and deletions in the VP1 region, and an isoleucine at the termination of the 3D polymerase[15,16,18,19]. The full sequence itself shares only 67–70% aligned nucleotide identity with other members of the HRV-C species and less than 60% with HRV-A and HRV-B strains.

After our recent complete genome sequencing of the known HRVs, we performed an alignment based on crystal structure superimposition and optimal energy RNA configurations, which we

Figure 2 HRV-C15 localization in sinus mucosa. (**a**) Sinus cultures were inoculated with medium alone (left) or HRV-C15 (center and right), and whole mounts of the tissue were analyzed for HRV-C15 RNA by *in situ* hybridization (purple stain). Scale bars, 1 mm. (**b**) Higher magnification view of the areas boxed in panel **a**, showing uninfected cells (left) or cells containing viral RNA (center and right). Scale bars, 0.15 mm. (**c**) Sections of mock- (left) or HRV-C–infected (center and right) sinus tissue. Right image is counterstained with eosin (pink). Scale bars, 15 µm.

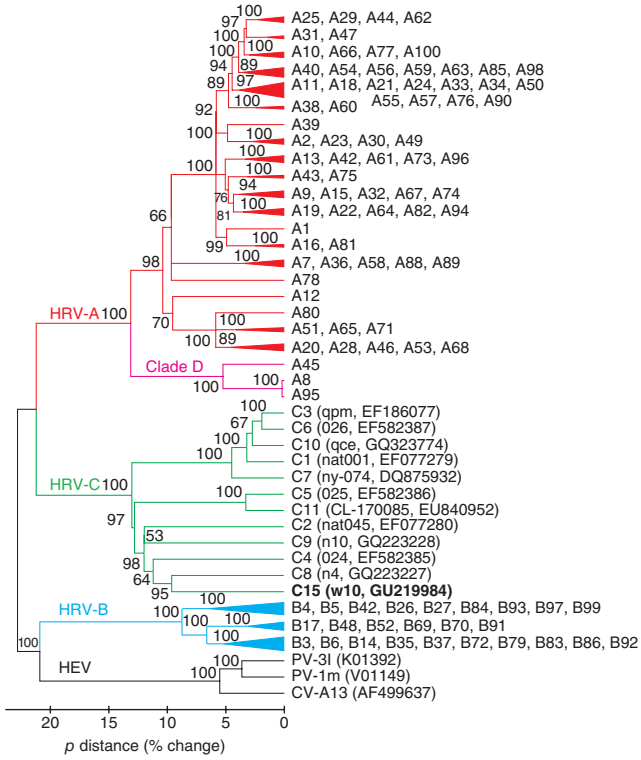

Figure 3 Neighbor-joining phylogenetic tree based on full-length nucleotide sequences of HRV-A, HRV-B and HRV-C. Complete 5′ and 3′ UTR sequences and the first and second codon positions of the open reading frames were considered (MEGA 4.1 software[35]). All major nodes are labeled with bootstrap values (% of 1,000 replicates). HRV-A and HRV-B reference strain accession numbers correspond to those published previously[1]. The HRV-C15 (W10) genome sequenced in this study is shown in bold type. Branch lengths are proportional to nucleotide similarity (*p* distance). Human enteroviruses (HEV) are included as an outgroup. HRV-C types (followed by strain designations and accession numbers) correspond to the recent classification proposal[31].

term a structure-based sequence alignment[1]. This data set was augmented with the HRV-C15 and other recently published HRV-C sequences[13,18,19] to infer phylogeny and establish species- or genus-specific motifs to predict cell attachment binding sites of HRV-C. A neighbor-joining tree calculated from the complete genomes (representing 74 HRV-A, 25 HRV-B and 12 HRV-C types) placed HRV-C15 in the HRV-C cluster on a branch most closely related to strain n4 (17% *p* distance), isolated in China in 2006 (**Fig. 3**); 5′ UTR analysis revealed HRV-Ca type[18] clustering (**Supplementary Fig. 1**). The available HRV-C sequences, including HRV-C15, show more collective diversity than the known types of HRV-A and HRV-B, suggesting there is still additional sequence space for other strains in this species.

HRV-C relative to ICAM-1 and LDLR footprints

Differences in overall capsid sequence together with the failure of HRV-C15 to replicate in standard cell lines suggest that HRV-C viruses have unique growth requirements, possibly including binding to distinct cellular receptors. Notably, HRVs have great plasticity and rapid evolution, as demonstrated by the adaptation of major-group HRV (A89) to use another receptor (heparan sulfate) for cell entry[20]. We were therefore interested in determining whether HRV-C has sequence consistency in the same sites as receptor footprints mapped for HRV-A and HRV-B[21–24].

For each alignment position harboring known contacts for ICAM-1 (HRV-B14, HRV-A16 or human coxsackievirus A21) or LDLR (HRV-A2), we recorded the group amino acid populations and then compared them (as groups or internally and pairwise, **Supplementary Tables 1** and **2**). When we compared the ICAM-1 binders among themselves, about 40% of identified footprint positions showed strong ($r > 0.6$) composition conservation (for example, Thr180 in VP3 of HRV-B14 (14-T-3-180)). Some of these positions were conserved among all HRVs (for example, B14-P-1-155 and A16-G-1-148). In contrast, other sites showed a compositional bias between receptor groups (for example, B14-P-3-178). **Figure 4a** depicts the most abundant residues at each footprint position when the HRV-A and HRV-B sequences were subdivided by ICAM-1 and LDLR receptor groups and compared to the HRV-C sequences. There was little commonality between HRV-C and either the ICAM-1 or the LDLR contact points. For example, six of seven LDLR footprint positions and 47 of 50 ICAM-1 footprint locations were rejected by both statistical methods as compositional matches to the HRV-C (**Supplementary Table 2**). Overall, the analysis predicts the HRV-C viruses use a different receptor with a distinct compositional footprint from HRV-A and HRV-B viruses.

Inhibition of HRV-C15 attachment

We then tested the distinct HRV-C receptor footprint prediction in cell culture, using antibodies to block attachment of HRV to ICAM-1 or LDLR. In the absence of these antibodies, binding of HRV-A1 and HRV-A16 to both HeLa and PBE cells was two to three logs higher compared to HRV-C15 (**Fig. 4b**,**c**). Preincubation of HeLa cells with an ICAM-1–specific antibody reduced binding of major-group HRV-A16 but not minor-group HRV-A1 (**Fig. 4b**). In cultures of PBE cells, only HRV-A1 was inhibited by preincubation with an LDLR-specific antibody (**Fig. 4c**). When the experiment was carried out with matched tissue snippets from sinus organ cultures, binding of HRV-C15 was similar to that of the other two viruses. Receptor-specific antibodies inhibited attachment of the respective major (80% inhibition) and minor (58% inhibition) viruses, but there was no effect on HRV-C15 binding (**Fig. 4d**).

HRVs have been divided into two groups (A and B) on the basis of their sensitivity to different antiviral compounds known as capsid-binding agents[25]. These compounds (for example, WIN56291 and WIN52084) intercalate into a hydrophobic pocket within the VP1 protein and prevent viral attachment or uncoating by deforming the receptor binding site or inhibiting a requisite conformational change[26–28]; thus the primary sequence dictating shape and charge of the pocket determine the response to specific antivirals. Preincubation of virus inoculums with WIN56291 inhibited propagation of HRV-A16 (group B) and HRV-C15, but not HRV-B14 (group A), in sinus organ culture (**Fig. 4e**).

Reverse genetics system for HRV-C

The results of the viral binding studies suggest that HRV-C15 does not replicate in HeLa and PBE cells, which are readily infected with HRV-A and HRV-B, because these cells do not express a cell surface receptor for the virus. Alternatively, these cells could lack an intracellular protein that is required for HRV-C replication. To test this hypothesis, we developed a plasmid (pC15) for cell transfection (as opposed to viral infection) by cloning a full-length cDNA copy of the HRV-C15 genome into the plasmid vector pMJ3 (ref. 29) directly downstream of the T7 RNA polymerase promoter (**Supplementary Fig. 2**). The cloned HRV-C15 sequence was identical to the complete genome sequence of passage four HRV-C15 (**Fig. 1d**) and contained a 3′-end poly(A_{29}) tail.

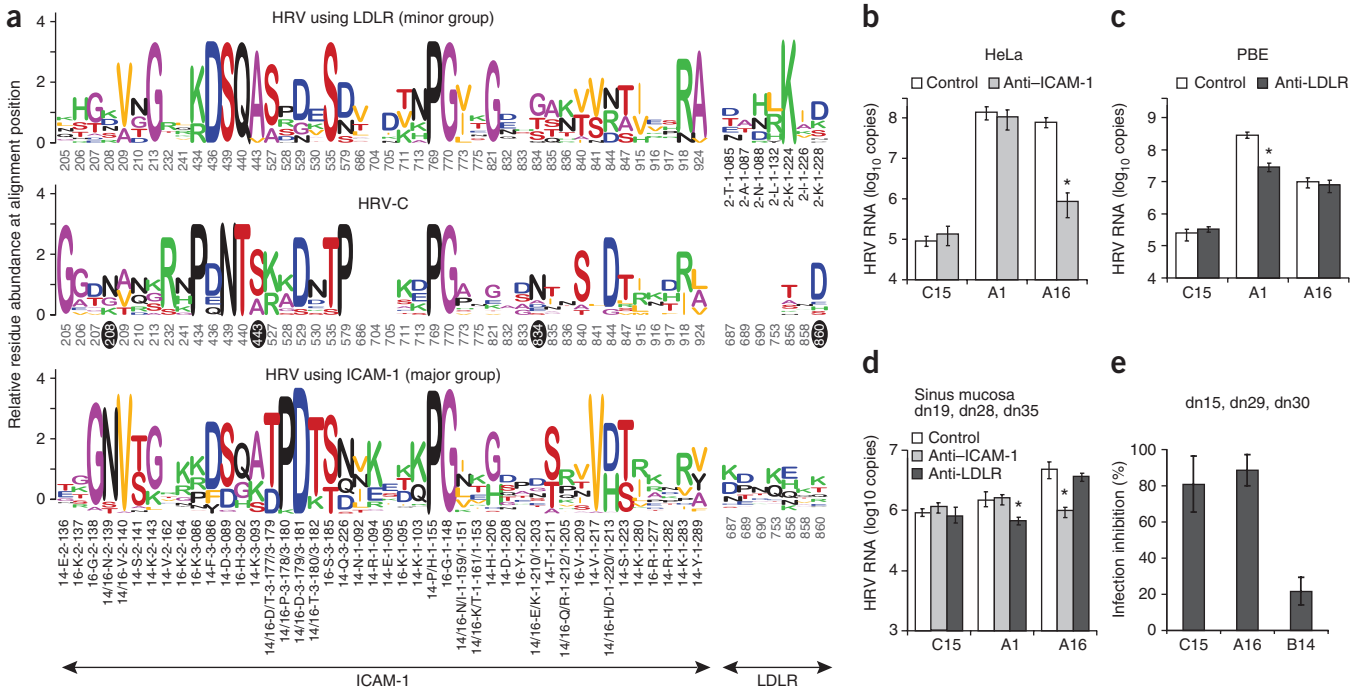

Figure 4 HRV-C composition at known receptor footprint sites, binding characteristics and drug sensitivity. (**a**) WebLogo[36] depiction shows the dominant amino-acid compositions at alignment positions with ICAM-1 (HRV-B14 or HRV-A16) or LDLR (HRV-A2) footprint contact residues. Human coxsackievirus A21-only locations are not shown. Positions are labeled either by alignment rank (for example, 205, 206 and so on), or by the structural name of the virus protein residue contributing to the footprint (for example, 16-G-1-148). Compositions were tabulated separately for minor-group (14 strains) or major-group (119 strains) HRV-A and HRA-B and HRV-C (11 strains). Alignment positions identified as compositional matches (circled) or mismatches (all others) to the HRV-C by Pearson or Spearman statistical analyses for each receptor footprint cohort are shown. (**b**–**d**) Inhibition of virus attachment in HeLa cells (**b**), PBE cells (**c**) or sinus mucosa (**d**) using receptor-blocking antibodies. Viral RNA was quantified in cell lysates and normalized to β-actin (*ACTB*) expression (means ± s.d., $n \geq 3$). *$P < 0.05$ versus medium control. (**e**) Inhibition of virus growth in sinus mucosa by WIN56291 (means ± s.d.).

RNA transcripts synthesized *in vitro* from pC15 induced cytopathic effects when transfected into both HeLa and WisL (fetal lung fibroblast) cell monolayers, and these effects were similar to those induced by parallel transfection of HRV-A16 RNA from pR16.11 (ref. 30) (**Fig. 5a**). After transfection of lower doses of RNA, only HRV-A16 RNA caused CPE progression over time, confirming that the newly synthesized HRV-C15 virus cannot spread from transfected cells to neighboring (not transfected) cells (**Supplementary Fig. 3**). We inoculated HRV-C15 virus recovered 24 h after transfection (1×10^9 vRNA copies per ml) into mucosal organ cultures, and the growth kinetics of progeny virus (**Fig. 5b**) was similar to those of the parental HRV-C15 (**Fig. 1e**). Examination of concentrated cell lysates by electron microscopy revealed intact HRV virions (about 30 nm in diameter) as well as the expected empty capsids (**Fig. 5c**).

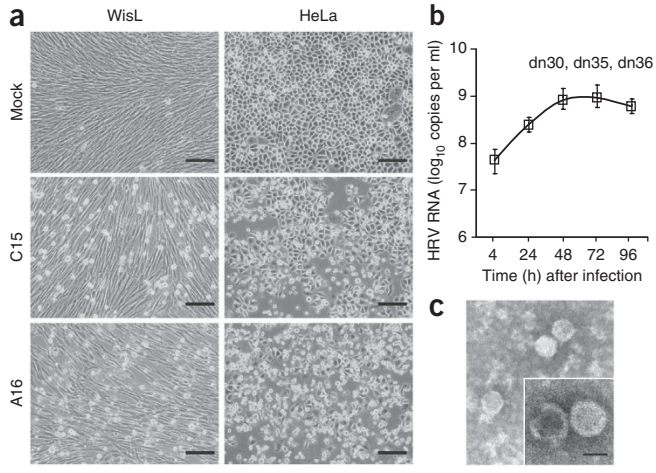

Figure 5 RNA transcripts derived from pC15 clone are infectious. (**a**) Cytopathic effects observed 24 h after transfection of WisL and HeLa cells with full-length HRV-A16 or HRV-C15 RNA. Scale bars, 100 μm. (**b**) Growth curve analysis of HRV-C15 progeny virus recovered after transfection of WisL cells. (**c**) Electron microscopy of concentrated cell lysates obtained 24 h after transfection of WisL cells with HRV-C15 RNA. Scale bar, 25 nm.

DISCUSSION

HRV-C viruses do not grow in standard cell culture used for virus isolation and have only been detected by molecular assays. Since 2006, over 60 types of this species have been implicated in both upper and lower respiratory tract infections, particularly in children and in individuals with chronic respiratory diseases[31]. We employed human organ culture of sinus mucosa to propagate *in vitro* and study the basic biologic properties of an HRV-C clinical isolate (C15 type). Virus replication was demonstrated by an increase in viral RNA, which localized to focal areas in epithelial cell layers. The high-titer virus obtained after serial passage in sinus organ culture allowed complete genome sequencing and cloning of the full-length cDNA copy of the HRV-C15 genome into a plasmid vector. RNA transcripts synthesized *in vitro* from this clone were infectious when transfected into cell lines resistant to HRV-C15 infection, providing an efficient system for production of recombinant HRV-C.

Our experimental findings and bioinformatic predictions indicate unique HRV-C receptor-binding specificity.

Mucosal organ culture is the only model to date that supports HRV-C infection *in vitro*. We and others have tried to grow these newly discovered rhinoviruses from numerous NLF samples in multiple cell cultures without success, indicating unique growth requirements[10,15,16]. Moreover, our attempts to adapt high-titer HRV-C15 virus grown in sinus cultures or recombinant virus from transfected cells to a cell line were not successful. HRV-C replication in sinus tissue seems to be limited to the epithelium, and hybridization signals were associated with both nonciliated and ciliated cells. The degree of virus amplification (high or low virus yields) showed considerable variability, which could be related to the condition of the epithelium (all specimens were from individuals with sinusitis), other underlying diagnoses (for example, allergy or asthma) or perhaps the status of local innate immune elements. Furthermore, the expression of HRV-C–specific receptors on epithelial cells may depend on factors found *in vivo* such as microbial products or interactions with other types of cells (for example, dendritic cells or lymphocytes) present in human airways.

Footprints of virus capsid residues that make contact with the cellular receptors have been determined for both major and minor HRV groups[21–24]. Sequence comparisons within the mapped receptor footprints show variability and a tendency toward a species-specific compositional bias among ICAM-1 binders[32]. However, amino acid residues corresponding to the documented ICAM-1 footprint have been shown to clearly classify the two receptor groups[33]. The LDLR binders are harder to define by sequence. They always have a conserved central lysine (for example, in HRV-A2 VP1 it is Lys224) , but this residue is not unique to LDLR binders, and predictive modeling instead suggests that the overall binding specificity primarily relies on a favorable combination of charge complementarities and hydrophobic interactions[34]. Comparisons of the group amino acid populations of the all known ICAM-1 or LDLR contact residues using two correlation metrics (Spearman and Pearson) revealed that the majority of footprint locations were rejected by both methods as compositional matches to the HRV-C, suggesting that an alternate receptor is used by these viruses. In agreement with this analysis, very low amounts of HRV-C15 attached to HeLa and PBE cells, and incubation of mucosal organ cultures with blocking antibodies to major and minor HRV receptors showed no effects on HRV-C15 binding.

The development of sinus organ culture and a reverse genetics system have enabled studies of HRV-C15 growth *in vitro* and have provided new insights into its unique replication cycle. HRV-C15 binds to an unknown receptor that is expressed on epithelial cells in differentiated tissues but is either absent or underexpressed in many cell lines and is clearly distinct from receptors used by other HRV species. It is possible that the lack of knowledge about the HRV-C receptor and the virus's biology has impeded the development of effective antivirals for HRV, as previous candidate medications were tested only against HRV-A and HRV-B viruses before moving into clinical trials. Even though not all enterovirus species have VP1 motifs that confer susceptibility to capsid binding agents, our results show that this approach can be used to block HRV-C binding and replication. Thus, these studies provide evidence that there are at least two feasible approaches to the treatment or prevention of HRV infections; refinement of capsid binding agents that target multiple species and development of competitive antagonists for the HRV receptors. The availability of organ culture and reverse genetics system should greatly facilitate further studies on HRV-C biology and its receptor identification.

METHODS

Methods and any associated references are available in the online version of the paper at http://www.nature.com/naturemedicine/.

Note: Supplementary information is available on the Nature Medicine website.

ACKNOWLEDGMENTS

We thank D. Heatley, G. Hartig and J.S. McMurray (University of Wisconsin–Madison) for providing surgical samples and R. Brockman-Schneider, R. Vrtis, T. Pappas, G. Crisafi, M. Hill, J. Bork, R. Massey, A. Lashua and E. Domyan for technical assistance. This work was supported by US National Institutes of Health grants U19 AI070503, U19 AI070503-04S1, R01 HL080412 and R01 HL091490 and the National Institute of Allergy and Infectious Diseases–funded University of Maryland School of Medicine Genome Sequencing Center for Infectious Disease.

AUTHOR CONTRIBUTIONS

Y.A.B. designed and performed experiments, analyzed data and was the principal author of the paper; A.C.P. performed sequence alignments, statistical receptor footprint analysis and contributed to writing; W.-M.L. performed partial sequencing of clinical isolates, constructed pW10-2R, designed antiviral compound experiments and provided purified HRVs; J.A.R. determined the complete genome sequence of HRV-C15; S.P.A. assisted with virus inhibition experiments; X.S. designed and assisted with *in situ* hybridization experiments; T.R.P. assisted with establishment of the sinus organ culture; N.N.J. and S.B.L. analyzed data and contributed to writing; J.E.G. designed the project, analyzed data and contributed to writing.

COMPETING FINANCIAL INTERESTS

The authors declare competing financial interests: details accompany the full-text HTML version of the paper at http://www.nature.com/naturemedicine/.

Published online at http://www.nature.com/naturemedicine/.
Reprints and permissions information is available online at http://www.nature.com/reprints/index.html.

1. Palmenberg, A.C. *et al.* Sequencing and analyses of all known human rhinovirus genomes reveal structure and evolution. *Science* **324**, 55–59 (2009).
2. Gern, J.E. & Busse, W.W. Association of rhinovirus infections with asthma. *Clin. Microbiol. Rev.* **12**, 9–18 (1999).
3. Hayden, F.G. Rhinovirus and the lower respiratory tract. *Rev. Med. Virol.* **14**, 17–31 (2004).
4. Dougherty, R.H. & Fahy, J.V. Acute exacerbations of asthma: epidemiology, biology and the exacerbation-prone phenotype. *Clin. Exp. Allergy* **39**, 193–202 (2009).
5. Jackson, D.J. *et al.* Wheezing rhinovirus illnesses in early life predict asthma development in high-risk children. *Am. J. Respir. Crit. Care Med.* **178**, 667–672 (2008).
6. Wat, D. *et al.* The role of respiratory viruses in cystic fibrosis. *J. Cyst. Fibros.* **7**, 320–328 (2008).
7. McManus, T.E. *et al.* Respiratory viral infection in exacerbations of COPD. *Respir. Med.* **102**, 1575–1580 (2008).
8. Lamson, D. *et al.* MassTag polymerase-chain-reaction detection of respiratory pathogens, including a new rhinovirus genotype, that caused influenza-like illness in New York State during 2004–2005. *J. Infect. Dis.* **194**, 1398–1402 (2006).
9. McErlean, P. *et al.* Characterisation of a newly identified human rhinovirus, HRV-QPM, discovered in infants with bronchiolitis. *J. Clin. Virol.* **39**, 67–75 (2007).
10. Lee, W.M. *et al.* A diverse group of previously unrecognized human rhinoviruses are common causes of respiratory illnesses in infants. *PLoS ONE* **2**, e966 (2007).
11. Briese, T. *et al.* Global distribution of novel rhinovirus genotype. *Emerg. Infect. Dis.* **14**, 944–947 (2008).
12. Mackay, I.M. *et al.* Prior evidence of putative novel rhinovirus species, Australia. *Emerg. Infect. Dis.* **14**, 1823–1824 (2008).
13. Tapparel, C. *et al.* Pneumonia and pericarditis in a child with HRV-C infection: a case report. *J. Clin. Virol.* **45**, 157–160 (2009).
14. Bizzintino, J. *et al.* Association between human rhinovirus C and severity of acute asthma in children. *Eur. Respir. J.* published online, doi:10.1183/09031936.00092410 (6 August 2010).
15. Lau, S.K. *et al.* Clinical features and complete genome characterization of a distinct human rhinovirus (HRV) genetic cluster, probably representing a previously undetected HRV species, HRV-C, associated with acute respiratory illness in children. *J. Clin. Microbiol.* **45**, 3655–3664 (2007).
16. McErlean, P. *et al.* Distinguishing molecular features and clinical characteristics of a putative new rhinovirus species, human rhinovirus C (HRV C). *PLoS One* **3**, e1847 (2008).
17. Arden, K.E. & Mackay, I.M. Newly identified human rhinoviruses: molecular methods heat up the cold viruses. *Rev. Med. Virol.* **20**, 156–176 (2010).

18. Huang, T. *et al.* Evidence of recombination and genetic diversity in human rhinoviruses in children with acute respiratory infection. *PLoS ONE* **4**, e6355 (2009).
19. Arden, K.E. *et al.* Molecular characterization and distinguishing features of a novel human rhinovirus (HRV) C, HRVC-QCE, detected in children with fever, cough and wheeze during 2003. *J. Clin. Virol.* **47**, 219–223 (2010).
20. Reischl, A. *et al.* Viral evolution toward change in receptor usage: adaptation of a major group human rhinovirus to grow in ICAM-1-negative cells. *J. Virol.* **75**, 9312–9319 (2001).
21. Olson, N.H. *et al.* Structure of a human rhinovirus complexed with its receptor molecule. *Proc. Natl. Acad. Sci. USA* **90**, 507–511 (1993).
22. Bella, J., Kolatkar, P.R., Marlor, C.W., Greve, J.M. & Rossmann, M.G. The structure of the two amino-terminal domains of human ICAM-1 suggests how it functions as a rhinovirus receptor and as an LFA-1 integrin ligand. *Proc. Natl. Acad. Sci. USA* **95**, 4140–4145 (1998).
23. Verdaguer, N., Fita, I., Reithmayer, M., Moser, R. & Blaas, D. X-ray structure of a minor group human rhinovirus bound to a fragment of its cellular receptor protein. *Nat. Struct. Mol. Biol.* **11**, 429–434 (2004).
24. Xiao, C. *et al.* Discrimination among rhinovirus serotypes for a variant ICAM-1 receptor molecule. *J. Virol.* **78**, 10034–10044 (2004).
25. Andries, K. *et al.* Two groups of rhinoviruses revealed by a panel of antiviral compounds present sequence divergence and differential pathogenicity. *J. Virol.* **64**, 1117–1123 (1990).
26. Oliveira, M.A. *et al.* The structure of human rhinovirus 16. *Structure* **1**, 51–68 (1993).
27. Zhao, R. *et al.* Human rhinovirus 3 at 3.0 A resolution. *Structure* **4**, 1205–1220 (1996).
28. Ledford, R.M. *et al.* VP1 sequencing of all human rhinovirus serotypes: insights into genus phylogeny and susceptibility to antiviral capsid-binding compounds. *J. Virol.* **78**, 3663–3674 (2004).
29. Lee, W.M., Monroe, S.S. & Rueckert, R.R. Role of maturation cleavage in infectivity of picornaviruses: activation of an infectosome. *J. Virol.* **67**, 2110–2122 (1993).
30. Lee, W.M. & Wang, W. Human rhinovirus type 16: mutant V1210A requires capsid-binding drug for assembly of pentamers to form virions during morphogenesis. *J. Virol.* **77**, 6235–6244 (2003).
31. Simmonds, P. *et al.* Proposals for the classification of human rhinovirus species C into genotypically assigned types. *J. Gen. Virol.* **91**, 2409–2419 (2010).
32. Rossmann, M.G. & Palmenberg, A.C. Conservation of the putative receptor attachment site in picornaviruses. *Virology* **164**, 373–382 (1988).
33. Laine, P., Blomqvist, S., Savolainen, C., Andries, K. & Hovi, T. Alignment of capsid protein VP1 sequences of all human rhinovirus prototype strains: conserved motifs and functional domains. *J. Gen. Virol.* **87**, 129–138 (2006).
34. Weber, C. *et al.* Predictive bioinformatic identification of minor receptor group human rhinoviruses. *FEBS Lett.* **583**, 2547–2551 (2009).
35. Tamura, K., Dudley, J., Nei, M. & Kumar, S. MEGA4: Molecular Evolutionary Genetics Analysis (MEGA) software version 4.0. *Mol. Biol. Evol.* **24**, 1596–1599 (2007).
36. Crooks, G.E., Hon, G., Chandonia, J.M. & Brenner, S.E. WebLogo: a sequence logo generator. *Genome Res.* **14**, 1188–1190 (2004).

ONLINE METHODS

Viruses. The virus nomenclature follows current recommendations of the International Committee on Taxonomy of Viruses *Picornaviridae* Study Group, designating the HRV species (A, B, C), followed by the assigned virus type (for example, HRV-A16, HRV-C15 and so on). We propagated laboratory stocks of HRV-A1 strain A (minor receptor group), HRV-A16 and HRV-B14 (major receptor group) in H1-HeLa cells (American Type Culture Collection CRL1958), and purified and titered as previously described[29,37]. HRV-A78 and HRV-C15 (previously designated W10) are clinical isolates that we identified by partial sequencing of the 5′ UTR as previously described[10].

Sinus mucosal organ culture. All protocols for these studies were reviewed and approved by the University of Wisconsin–Madison Health Sciences Institutional Review Board. We obtained residual airway tissue specimens from individuals with chronic sinusitis undergoing endoscopic surgery (informed consent was not required, as the specimens would otherwise have been discarded after surgery). We washed, sectioned (4 × 4 mm) and submerged snippets of epithelium along with underlying tissues individually in 24-well plates with 0.3 ml bronchial epithelial growth medium (BEGM, Lonza) and incubated them at 37 °C (5% CO_2). Before use, we tested all specimens for pre-existing respiratory viruses, including HRV, adenoviruses, influenza, parainfluenza, enteroviruses, respiratory syncytial virus, metapneumovirus, coronaviruses and bocavirus (Respiratory Multi-Code PLx Assay, EraGen Biosciences)[38].

HRV-C infection of mucosal organ culture. We washed tissue squares (four or five per well) with PBS (three washes with 0.5 ml) before inoculation (2×10^8 vRNA copies per ml) with a virus suspension. After a period of collective incubation (4–6 h, 34 °C, 5% CO_2) we aspirated the medium and redistributed the individual tissue samples into separate wells with fresh BEGM (0.3 ml) for further incubation (72–96 h). At collection time, we exposed the combined medium and tissue from each well to one freeze-thaw cycle, clarified them by low-speed centrifugation (3,000*g*, 5 min), then passaged with fresh tissue snippets or aliquoted and stored (−80 °C).

Virus detection and quantification. We evaluated virus concentration by SYBR Green qRT-PCR reagents (Applied Biosystems) with primers (forward, 5′-CCTCCGGCCCCTGAAT-3′; reverse, 5′-AAACACGGACACCCAAAGTAGT-3′) that were complementary to the 5′ UTR of HRV-A1, HRV-A16, HRV-B14 and HRV-C15. We used primers and probe for *ACTB* (4326315E, Applied Biosystems) to normalize RNA content in cell and tissue lysates. We isolated total RNA from 100 µl of growth medium or mucosal tissue (RNeasy Mini Kit, Qiagen), reverse-transcribed it (TaqMan, Applied Biosystems) and performed PCR in duplicate (ABI 7000 Real-Time PCR System, Applied Biosystems). We derived the standard curve from purified HRV-C15 RNA transcripts synthesized *in vitro*. We performed melting curve analysis of the amplicons after each PCR to confirm reaction specificity.

RNA *in situ* hybridization. We cloned a cDNA fragment (867 bases) of HRV-C15, encoding the 5′ UTR (partial), VP4 and partial VP2 genes into plasmid pMJ3 (ref. 29) after a T7 RNA polymerase promoter in reverse orientation to create plasmid pW10-2R. T7-induced transcription of linearized pW10-2R produced digoxigenin-labeled (Roche) probes that detect the viral genome RNA. We fixed, processed and hybridized sinus tissue samples according to described protocols[39,40]. Additional details are provided in the **Supplementary Methods**.

Inhibition assays. We preincubated cultured cells or tissue samples (30 min, 37 °C) with monoclonal ICAM-1–specific (BBA3) or polyclonal LDLR-specific (AF2148) antibodies (R&D Systems) diluted in growth medium (10 µg ml^{-1}) or medium alone (control). Next, we added a virus suspension of 2×10^8 vRNA copies per well containing either mucosal organ culture or PBE cell monolayers (six-well plate) or per tube containing 1×10^6 HeLa cells in suspension. We incubated cells or tissues with the virus (1 h, 25 °C), washed three times and analyzed by qPCR. To test the efficacy of the capsid-binding compound WIN56291 (Sterling Winthrop), we incubated (30 min, 25 °C) virus samples (2×10^8 vRNA copies) in 0.1 ml BEGM containing the compound (0.5 µg ml^{-1}, 0.1% DMSO), followed by inoculation (5 h, 34 °C) into sinus organ cultures. After aspirating unattached virus, we incubated tissues for 72 h and tested by qPCR.

Construction of the full-length cDNA copy of HRV-C15. We isolated total RNA (RNeasy Mini Kit, Qiagen) from 100 µl of organ culture supernatant (HRV-C15 passage 4). After reverse transcription with random primers (TaqMan, Applied Biosystems), we performed PCR with the Platinum PCR SuperMix HF (Invitrogen) and primers (**Supplementary Table 3**). The strategy for cloning the full-length cDNA copy of HRV-C15 is described in **Supplementary Figure 2**. We confirmed each viral cDNA insert by automated sequencing of both strands.

RNA transfection. We purified full-length RNA transcripts synthesized from the linearized (BstBI) pC15 DNA (RiboMax large-scale RNA production system T7, Promega) with an RNeasy Mini Kit (Qiagen) and analyzed by agarose gel electrophoresis. We transfected cells with RNA and Lipofectamine 2000 (Invitrogen) mixture (1 to 5 wt/vol ratio) using the manufacturer's recommendations and incubated for 24–72 h. See the **Supplementary Methods** for a detailed protocol.

Statistical analysis. We used Student's *t* test to analyze viral replication data (SigmaPlot 11.0, Systat Software). Significance was defined at $P < 0.05$. Statistical evaluation of HRV receptor footprints is described in the **Supplementary Methods.**

37. Lee, W.M., Wang, W. & Rueckert, R.R. Complete sequence of the RNA genome of human rhinovirus 16, a clinically useful common cold virus belonging to the ICAM-1 receptor group. *Virus Genes* **9**, 177–181 (1995).
38. Lee, W.M. *et al.* High-throughput, sensitive, and accurate multiplex PCR-microsphere flow cytometry system for large-scale comprehensive detection of respiratory viruses. *J. Clin. Microbiol.* **45**, 2626–2634 (2007).
39. Henrique, D. *et al.* Expression of a Delta homologue in prospective neurons in the chick. *Nature* **375**, 787–790 (1995).
40. Neubüser, A., Peters, H., Balling, R. & Martin, G.R. Antagonistic interactions between FGF and BMP signaling pathways: a mechanism for positioning the sites of tooth formation. *Cell* **90**, 247–255 (1997).